[Working title]: Intraspecific variation in range-wide seed bank dynamics is not consistent with density-independent model of bet hedging

Gregor-Fausto Siegmund and Monica Geber

Last updated: March 22, 2021

Introduction

Seed banks can buffer plant populations against environmental change and stochasticity (Eager et al. (2014); Paniw et al. (2017)), increase effective population size (Nunney (2002); Waples (2006)), and maintain genetic diversity (Mccue and Holtsford (1998)). Dormancy can affect the outcome of evolution (Heinrich et al. (2018); Ritland (1983)). Theory thus suggests that seed banks have ecological and evolutionary consequences (Evans and Dennehy (2005)).

What drives the evolution of delayed germination? The theory developed by Cohen (1966) frames the problem in the following terms. What is the optimal germination fraction for a given level of interannual variation in fitness and seed survivorship? These models make it clear that the germination fraction that maximizes long-term population growth rate is a function of the distribution of fitness (characterized by the variation in fitness), the fitness values, and the rate of seed survivorship. For a given mean fitness, increasing the variance in fitness decreases the optimal germination fraction. Increasing seed survivorship decreases the optimal germination fraction, and the degree to which it does so depends on the probability of a 'good year'. Specifically, as the probability of a high-fitness year decreases, the optimal germination fraction decreases. Bet hedging should evolve to maximize the long-term geometric population growth rate (as compared to the arithmetic population growth rate) (Cohen (1966, 1968); Ellner (1985*a*,*b*)).

Population vital rates are known to exhibit intraspecific variation across *Clarkia xantiana*'s geographic range, including age-specific germination and seed survival (Eckhart et al. (2011)). In a study of *C. xantiana* population dynamics that identified a decline of long-term stochastic population growth rate from west to east across the range, Eckhart et al. (2011) inferred a decrease in survival through winter (s_1) and an increase in germination rate (g_1) of first-year seeds from west to east. Although, Lewis 1962 suggested that *Clarkia*

populations undergo local extinctions and lack a long-lived seed bank, observations of 20 populations across the range are not consistent with that hypothesis (Figure 2). Demographic observations Eckhart et al. (2011) and transplant experiments demonstrate that fitness can exhibit dramatic interannual variation (e.g. 30-fold between a wet and dry year in Geber and Eckhart 2005).

Seed dormancy and persistence in the soil seed bank may be a bet-hedging strategy that is favored by environmental uncertainty. If this is the case in *C. xantiana*, we might expect increased seed survival and decreased germination probabilities in populations with more variability in per-capita reproductive success. However, broad geographic patterns in rainfall variability and life history are not consistent with this cursory explanation since variation in rainfall increases from west to east, and germination probability also increases Eckhart et al. (2011). We thus sought to understand intraspecific variation in *C. xantiana* seed vital rates in the context of broader life history patterns.

Bet hedging should evolve to maximize the long-term geometric population growth rate (as compared to the arithmetic population growth rate) (Cohen (1966, 1968); Ellner (1985*a*,*b*)). Seed banks are more likely to be selected in populations which experience higher levels of interannual variation in per-capita reproductive success. To investigate this empirical relationship, we estimate the correlation between germination and seed survival, and between germination variance in per-capita reproductive success. We also examined whether observed levels of germination are consistent with germination levels predicted by a density-independent model of bet hedging.

1 Methods

1.1 Clarkia life history

Clarkia xantiana is a winter annual that germinates with late fall and winter rains. In our study region, the Kern Valley in the southern Sierra Nevada Mountains, historically happens between October and late February or early March. Seedlings grow throughout the winter and spring, and surviving plants flower in late spring and early summer, April into early July. Pollinated fruits set seed in the early summer, June to July. Seeds of *C. xantiana* are produced in early summer, with fruits that dry out and gradually split open. Most seeds appear to be shed from fruits within 3-4 months after production, but can remain on the plant for up to a year. Seeds are small (< 1 mm in width) and have no structures to aid in aerial dispersal.

We represent the *Clarkia xantiana* as a life cycle graph (Figure 1A) that describes transitions from October of year t to October of year $t + 1$ in terms of underlying vital rates. The census period occurs when the entire population is seeds, and corresponds to the time at which seed bags are placed into the field (see below). Seeds are grouped into three stages: age 0 seeds, which were produced in the current year; age 1 seeds, which were produced in the previous year; age 2+ seeds, which were produced two or more years ago. Persistence of seeds in the seed bank is represented by transitions from younger to older seeds. Production of new seeds is captured by transition to the age 0 seed state.

Transitions in the life cycle graph are the product of age-specific seed survival and germination, and aboveground seedling survival to fruiting, fruit production, and seeds per fruit. Seed-related rates are represented separately for age 0, 1, and 2+ seeds. Germination for each age class is given as g_1, g_2, and g_3, respectively. Seed survival from seed production to the first October is given as s_0, and survival from October to February is given as s_1, s_3, and s_5 for age 0, 1, and 2+ seeds, respectively. Survival from February to October is given

as s_2, s_4, and s_6 for age 0, 1, and 2+ seeds, respectively. We assume that vital rates remain unchanged after age 2. We also we assume that all plants experience the same vital rates upon germination seed age at germination does not affect seedling survival to fruiting (σ), fruits per plant (F), or seeds per fruit (ϕ).

The life cycle graph (Figure 1A) corresponds to the annual projection matrix

$$\boldsymbol{A} = \begin{bmatrix} s_1 g_1 \sigma F \phi s_0 & s_3 g_2 \sigma F \phi s_0 & s_5 g_3 \sigma F \phi s_0 \\ s_1(1-g_1)s_2 & 0 & 0 \\ 0 & s_3(1-g_2)s_4 & s_5(1-g_3)s_6 \end{bmatrix} \tag{1}$$

that summarizes transitions between stages.

1.2 Creating the dataset

We used field experiments and surveys to assemble observations of below- and above-ground demography for 20 populations of *Clarkia xantiana* (Table 1). Specifically, we used experiments to estimate transitions in the seed bank and surveys to estimate components of per-capita reproductive success. These demographic data have previously been used to test hypotheses about the geography of demography (Eckhart et al. 2011) and species distributions (Pironon et al. 2018). Here, we sought to obtain population-level estimates of germination and seed survival, and yearly estimates of per-capita reproductive success.

To estimate transitions in the seed bank, we used observations from a seed bag burial experiment conducted in all populations from 2006-2009 (Figure 3). The experiment has been previously described in Eckhart et al. 2011 and we reanalyze the data here. Geber and collaborators buried seeds in bags and unearthed 1, 2, or 3 years after being buried to count seedlings and intact, viable seeds. The experiment was repeated in 3 consecutive years and ended in 2009. We thus have 3 sets of observations associated with 1 year old seeds, 2 sets

of observations associated with 2 year old seeds, and 1 set of observations associated with 3 year old seeds. We use data from the experiment to estimate age-specific germination and seed survival (see Joint model for seed vital rates) but note that we test predictions of bet-hedging theory that are based on an unstructured seed bank and use only the relevant subset of transitions in our analysis (see Computing vital rates).

To estimate per-capita reproductive success, we combine censuses of seedlings and fruiting plants, surveys of fruits per plant, and lab counts of seeds per fruit. To assess the survival of seedlings to fruiting plants, we counted seedlings and fruiting plants in 30 0.5 m^2 permanent plots from 2006–2018 (Eckhart et al. 2011). To assess seed production by plants that survive to reproduction, we counted fruits per plant on individual plants in permanent plots, and on additional haphazardly chosen plants throughout the population. We then attempted to obtain 20-30 fruits per population, which we used to count seeds per fruit (Eckhart2011).

Table 1: Summary of data sets used to estimate parameters.

Parameter data	Description	Data set	Time span
SEED VITAL RATES	—	—	—
Seed survival and germination	Seed bag burial	$\mathbf{Y}_1$	2006-2009
Seed viability	Viability trials	$\mathbf{Y}_2$	2006-2009
SEEDLING SURVIVAL	—	—	—
Seedling survival to fruiting	Field surveys	$\mathbf{Y}_4$	2006-2019
FRUITS PER PLANT	—	—	—
Total fruit equivalents per plant	Field surveys	$\mathbf{Y}_5$	2006-2012
Undamaged and damaged fruits per plant	Field surveys	$\mathbf{Y}_6$	2013-2019
Total fruit equivalents per plant	Extra plots	$\mathbf{Y}_7$	2006-2012
Undamaged and damaged fruits per plant	Extra plots	$\mathbf{Y}_8$	2013-2019
SEEDS PER FRUIT	—	—	—
Seeds per undamaged fruit	Lab counts	$\mathbf{Y}_9$	2006-2019
Seeds per damaged fruit	Lab counts	$\mathbf{Y}_{10}$	2013-2019

1.3 Model

We use observational and experimental data from 20 populations of *Clarkia xantiana* to estimate transition probabilities across the life cycle. We fit multilevel models to obtain

population-specific estimates for belowground vital rates, and year- and population-specific estimates for aboveground vital rates. Because we were interested in describing the life histories of individual populations, we built separate models for each population. Our general approach applies a common model structure to partially pool observations from each population.

We first explicitly describe our formulation in terms linear mixed models before defining the joint posterior (Evans et al. 2010, Ogle and Barber 2020). We assume that the latent mean of observations in year j at a population k, θ_{jk}, is drawn from a normal distribution with mean $\theta_{0,k}$ and variance σ_j^2.

$$\theta_{jk} = \theta_{0,k} + \epsilon_{(jk)}. \tag{2}$$

Our model includes a population-level intercept $\theta_{0,k}$ and random effects $\epsilon_{(jk)}$. The random effects can be written as $\epsilon_{(jk)} \sim N(0, \varsigma^2)$. For the moment, we focus on describing the hierarchical structure of the model but note that we use link functions for transformation to parameters that are appropriate for the likelihoods we use to model different sets of observations (e.g. binomial for seed bag experiments; Poisson for counts of seed per fruit). We note that such a linear mixed effects model with random intercepts for years is one method commonly used to model interannual variation in demographic rates (e.g. Metcalf et al. 2015). Using hierarchical centering, the same model is rewritten as

$$\theta_{jk} = \alpha_{(jk)}. \tag{3}$$

The mean θ_{jk}, is now drawn from a normal distribution with mean $\alpha_{(jk)}$ and variance

σ_j^2. We place a prior on $\alpha_{(jk)}$ such that $\alpha_{(jk)} \sim N(\theta_{0,k}, \varsigma^2)$. The expressions are related by $\alpha_{(jk)} = \theta_{0,k} + \epsilon_{(jk)}$. We thus draw year-level means from the population-level means.

For a single population (ie. suppressing subscript k), we write the the posterior proportional to the joint distribution as

$$[\theta_j, \theta_0, \sigma_j^2, \varsigma^2 | y_{ij}] \propto [y_{ij}|\theta_j, \sigma_j^2][\theta_j|\theta_0, \varsigma^2][\theta_0][\sigma_j^2][\varsigma^2]. \tag{4}$$

The distribution of the observations y_{ij} is conditional on the year-specific parameters θ_j and σ_j^2. In turn, the year-specific parameter θ_j is conditional on the population-specific parameters θ_0 and ς^2. We placed priors on all parameters found only on the right hand side of conditional statements $(\theta_0, \sigma_j^2, \varsigma^2)$. In practice, we implemented this model by specifying the population- and year-levels of the model with normal distributions; for example, $[\theta_j|\theta_0, \varsigma^2]$ is $\theta_j \sim N(\theta_0, \varsigma^2)$. The model thus describes a structure in which years are nested within populations.

1.4 Model statements, implementation, and fitting

We include the expression for the posterior proportional to the joint distribution, and corresponding directed acyclic graphs, in Appendix: Joint Posterior. Priors for all parameters are defined in Table Priors. We applied the following principles for specifying priors: (1) we used weakly informative priors that avoided placing probability mass on biologically implausible values (Gelman; Lemoine; Wesner and Pomeranz), (2) we placed positive, unbounded priors on variance components (REF), (3) we conducted prior predictive checks to assess the scale of priors after parameter transformation (Hobbs and Hooten; Gabry; Wesner and Pomeranz), and (4) we simulated prior predictive distributions to confirm that the joint likelihood generated data within the observed range (Gabry; Conn; Hobbs and Hooten). We provide

additional detail regarding our choice of priors in Appendix: Priors.

We prepared data for analysis using the tidyverse and tidybayes packages (CITE) in R VERSION; CITE. We wrote, fit all models, and estimated posterior distributions using JAGS VERSION with rjags (Plummer 2016). We randomly generated initial conditions for all parameters with a prior by drawing from the corresponding probability distribution in R before passing the initial values to rjags. We ran three chains for XX,000 iterations. The first XX,000 samples were discarded as burn-in and we sampled the following XX,000 iterations. We did not thin the chains (Elderd and Miller 2016).

We assessed convergence of the MCMC samples with visual inspection of trace plots, by calculating the Brooks-Gelman-Rubin diagnostic (R-hat), and by calculating the Heidelberg-Welch diagnostic (Elderd and Miller 2016. The Gelman-Rubin diagnostic is used to assess convergence between chains and the Heidelberg-Welch for stationarity within chains. Trace plots for all chains, histograms of R-hat, and the percentage of chains that passed the HW test are shown in the appendix.

To evaluate our model's fit to the data, we performed model checks that are described in full in Appendix: Model Checking. We used our posterior distribution to simulate replicate datasets based on the parameters of our model. We compared samples from the simulated datasets to the real, observed datasets using both graphical, visual checks and by calculating Bayesian p-values for test statistics calculated for the observed and simulated data. In the following section, we describe how we used the models we fit to obtain the parameters that describe the *Clarkia* life history. While we do not perform model checks for these derived quantities (e.g. winter seed survival accounting for the combined effect of seed decay and loss of viability) because we combine the output of multiple models, the model checks are still essential to determine whether our inferences are reasonable.

1.5 Computing vital rates

1.5.1 Belowground vital rates

We used the age-specific germination probabilities, survival function, and viability estimates to account for viability in estimates for the probability of germination and survival. We first discretized the survival function to times at which we observed germination and counted seeds (January and October). Estimates of survival over these intervals are the probability that a seed remains intact, but does not account for loss of viability. Next, we used viability estimates from October to calculate viability for January by interpolation (Figure 3D). We tested the viability of seeds in October, and were thus able to estimate the proportion of viable seeds (Figure 3B; filled points). We inferred the viability of intact seeds in January by assuming that seeds lost viability at a constant rate (exponential decay). Further, we interpolated between estimates by assuming that viability changed at a constant rate between years, and that all seeds were viable at the start of the experiment (Figure 3B; open points).

We combined the discretized survival function and viability estimates to construct a survival function for the probability that a seed remains intact and viable (Table 2, column X). Specifically, we multiplied the posteriors of the discretized survival and viability estimates. Because we combined estimates, some portions of the posterior for seed survival probability was than 1, especially for later seed ages. We restricted the posterior to be less than 1 by truncating the distribution and resampling to redistribute the probability mass. We take this step to retain parameter uncertainty about survival probability in cases where combining the estimates implies a high probability of survival. The survival function for viable seeds (ϕ) is composed of estimates of persistence over time ($\theta_.$), estimates of viability ($\nu_.$), and estimates of germination conditional on persistence ($\gamma_.$).

We used the discretized survival function and age-specific germination probability to obtain the estimates of germination and seed survival required to test predictions from bet-

hedging theory. Table **??** defines the age-specific germination probabilities and survival probabilities for the structured model in Eckhart et al. 2011 in terms of the survival function and age-specific germination probabilities. Figure 3E-F illustrate the relationship among the various probabilities of germination and seed survival. Estimates from the seed bag experiment correspond to the probability of germination or survival conditional on persistence (e.g. γ_1). Multiplying these estimates by the probability of persistence up to a certain time gives the unconditional probability (e.g. $\theta_1 \times \gamma_1$). Finally, the probability conditional on persistence and viability is estimated by incorporating loss of viability into the survival function (e.g. γ_1/ϕ_1), and defines the parameters in the structured population model.

Table 2: Seed persistence and viability in the soil seed bank

	Persistence	Persistence & viability
Time (x_i)	$S(x_i)$	$S(x_i)$
Oct_0	θ_0	$\phi_0 = \theta_0$
$\text{Jan}_{1,\text{total}}$	θ_1	$\phi_1 = \theta_1(\gamma_1 + (1-\gamma_1)\nu_1^{1/3})$
$\text{Jan}_{1,\text{intact}}$	θ_2	$\phi_2 = \theta_2\nu_1^{1/3}$
Oct_1	θ_3	$\phi_3 = \theta_3\nu_1$
$\text{Jan}_{2,\text{total}}$	θ_4	$\phi_4 = \theta_4(\gamma_2 + (1-\gamma_2)\nu_1(\nu_2/\nu_1)^{1/3})$
Description	Parameter	Probability
July-October	s_0	
October-January	s_1	ϕ_1
1-year old germination	g_1	γ_1/ϕ_1
January-October	s_2	ϕ_3/ϕ_2
October-January	s_3	ϕ_4/ϕ_3

1.5.2 Per-capita reproductive success

In order to make our analysis comparable to previous empirical studies of bet hedging, we calculated per-capita reproductive success as the product of the probability of seedling survival to fruiting, fruits per plant, and seeds per fruit. We thus calculate per-capita reproductive success as the number of seeds produced per seedling, on average (e.g. Venable

2007, Gremer et al. 2014).

We used a consistent method to estimate seedling survival to fruiting throughout the experiment, and use the population- and year-level means ($\mu_{\mathrm{S},jk}$) in our calculation. Because we estimated fruit production in 2 different ways during the study, we chose to use total fruit equivalents (TFE) per plant as our common estimate of fruit production. From 2006–2012, we used $\mu_{\mathrm{TFE},jk}$) as estimated in the statistical model. From 2013–2018, we used the ratio of seeds per damaged to undamaged fruit to calculate a proportion of damaged fruits to add to undamaged fruit counts, as in

$$\mathrm{TFE} = \text{undamaged fruits} + \frac{\text{seeds per damaged fruit}}{\text{seeds per undamaged fruit}} \times \text{damaged fruits}. \tag{5}$$

We used posterior distributions for population- and year-level parameters (e.g. $\mu_{\mathrm{US},jk}$) for these calculations and obtained estimates of $\mu_{\mathrm{TFE},jk}$) for 2013–2018. Finally, we used estimates of seeds per undamaged fruit ($\mu_{\mathrm{US},jk}$) as our estimate of seeds per fruit.

In terms of parameters from our statistical models, per-capita reproductive success F_{jk} at population j in year k is calculated as

$$F_{jk} = \phi_{jk} \times \lambda_{\mathrm{TFE},jk} \times \lambda_{\mathrm{US},jk}, \tag{6}$$

where

$$\begin{aligned} \phi_{jk} &= \text{logit}^{-1}(\mu_{\text{S},jk}) \\ \lambda_{\text{TFE},jk} &= \exp(\mu_{\text{TFE},jk}) \\ \lambda_{\text{US},jk} &= \exp(\mu_{\text{US},jk}). \end{aligned} \tag{7}$$

Our multilevel models for aboveground vital rates pooled data more strongly in years with relatively little data. A benefit of this approach is that it implicitly corrects for variation in sample size (e.g. an observation of 0/37 seeds surviving is given more weight than an observation of 0/1 seeds surviving). While this is beneficial for distinguishing between spurious estimates and true temporal variation in reproductive success, it may also underestimate variation in reproductive success. At the extreme, estimates in years without any data are pooled to the population-level means. Years with zero seedling survivorship would thus have estimates for fruits per plant that are pooled towards the population-mean (because there were no fruiting plants on which to count fruits). We thus also considered a second estimate of reproductive success in which we assumed years in which we observed no plants had a per-capita reproductive success of 0.

Analysis

Correlation between germination probability and seed survival

Increased seed survivorship is predicted to decrease the optimal germination probability Cohen (1966); Ellner (1985*a*). I assessed whether the observed germination probability was negatively correlated with seed survival (Gremer and Venable (2014)). I calculated the probability that seeds which do not germinate in January remain in the seed bank until the following January ($s_2 s_3$). I obtained the posterior distribution for the correlation between germination and seed survival by calculating the correlation of g_1 and $s_2 s_3$ at each iteration

of the MCMC output Hobbs and Hooten 2015, p 194-5. Results of this analysis are shown in Figure 4. Bet hedging models predict that germination probability should be negatively correlated with seed survival; 95% credible intervals that do not overlap zero provide support for this prediction. The bottom panel shows the posterior distribution of correlation between the probability of germination and seed survival.

Correlation between germination probability and variance in per-capita reproductive success

Increased variance in per-capita reproductive success is predicted to decrease the optimal germination probability (Cohen (1966); Ellner (1985*a*)). I assessed whether the observed germination probability was negatively correlated with variance in per-capita reproductive success (Venable (2007)).

To calculate the temporal variation in per-capita reproductive success for each population, I sampled the posterior distribution of reproductive success for each year and calculated the geometric SD of per capita reproductive success. I obtained the sample correlation of germination and geometric SD of per capita reproductive success at each iteration of the MCMC output Hobbs and Hooten 2015, p 194-5. Bet hedging models predict that germination probability should be negatively correlated with temporal variance in fitness; 95% credible intervals that do not overlap zero provide support for this prediction. The geometric SD of per capita reproductive success was calculated as exp(SD (log (per capita reproductive success+0.5))) (Venable (2007)). Results of this analysis are shown in Figures 5 and 6.

Density-independent model for germination probability

We use estimates of seed survival and reproductive success to investigate the adaptive value of delayed germination (Gremer and Venable (2014)). We parameterize a model of population

growth rate and calculate the optimal germination strategy for different combinations of seed survival and reproductive success. We describe *C. xantiana*'s life cycle and calculate population growth rate with the equation:

$$\lambda = g_1 Y(t) s_0 s_1 + (1 - g_1) s_2 s_3 \tag{8}$$

Seed survival rates (s_0, s_1, s_2, s_3) are population-level estimates. Per capita reproductive success ($Y(t)$) is calculated as the product of seedling survival to fruiting, fruits per plant, and seeds per fruit (equation (6)). Temporal variation is incorporated into the model by varying the per-capita reproductive success, $Y(t)$, between years.

For each population, I numerically calculate the optimal germination probability for the observed variation in reproductive success and seed survival. In each case, I use the posterior mode of the parameter estimates in the equation for density-independent growth (equation (8)). I resampled the posterior modes of per-capita reproductive success ($Y(t)$) to obtain a sequence of 1000 years. I used this same sequence of $Y(t)$ and the seed survival probabilities to calculate long-term stochastic population growth rates (λ_s) at each germination probability along an evenly spaced grid of possible germination probabilities (G) between 0 and 1. The optimal germination probability is estimated as the value of G that maximizes the geometric mean of the population growth rate. I repeat the simulations 50 times for each population, resampling the sequence of per-capita reproductive success, $Y(t)$, each time. I then calculated the mean of the optimal germination fractions.

Models in which per-capita reproductive success is density-independent predict that germination probability should respond to variance in fitness (Cohen (1966)). To evaluate the density-independent model, I compared modeled germination probabilities to predicted germination optima. I plot this comparison in Figure 5 and 6. The dotted line indicates a 1:1 relationship between observations and predictions. Values below the line indicate that the

model predicts higher germination probabilities than observed; values above the line would indicate that the model predicts lower germination probabilities than observed.

Results

Correlation between germination probability and seed survival

I examined the correlation between germination probability and seed survival in the seed bank. Results of this analysis are shown in Figure 4. The bottom panel shows the posterior distribution of correlation between modeled germination probability and the probability of seed survival; the 95% credible interval for the correlation overlaps 0, suggesting that there is no correlation between germination and seed survival.

Correlation between germination probability and variance in per-capita reproductive success

I examined the correlation between germination probability and variance in per-capita reproductive success. Results of this analysis are shown in Figure 5 and 6. The bottom left panel shows the posterior distribution of correlation between modeled germination probability and geometric SD in per-capita reproductive success. Setting years without any observed plants to have a fitness of zero increases the range of the geometric standard deviation in reproductive success (compare panels A in Figure 5 and 6). However, for both calculations of per capita reproductive success, the median correlation is slightly positive and the 95% credible interval overlaps 0.

Optimal germination probability predicted by a density-independent model

Optimal germination probabilities were less than 1 in all populations when we assumed that years without plants had zero fitness, but not when we used the partially pooled estimates

of per-capita reproductive success (Figure 5 and 6). In both cases, predictions from the density-independent model overestimated the probability of germination (points fall below the 1:1 line).

Discussion

...

Figures

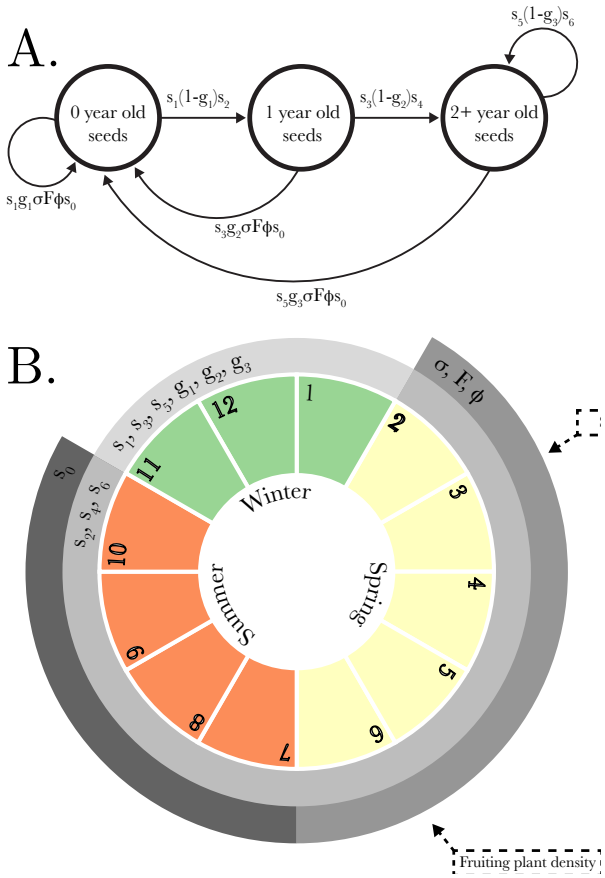

Figure 1: Diagram representations of Clarkia life cycle. Note: Bottom panel needs to be edited so that the dotted lines on the outside of the figure are removed.

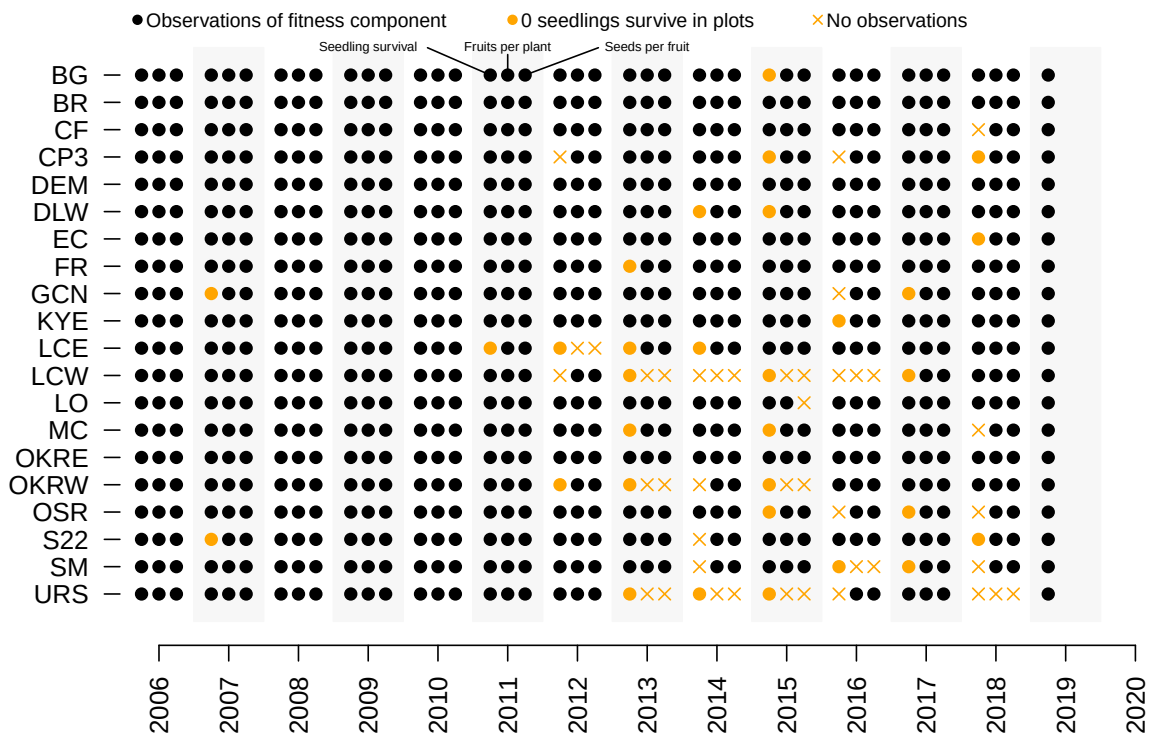

Figure 2: Summary of the aboveground observations, low fitness, and no observations.

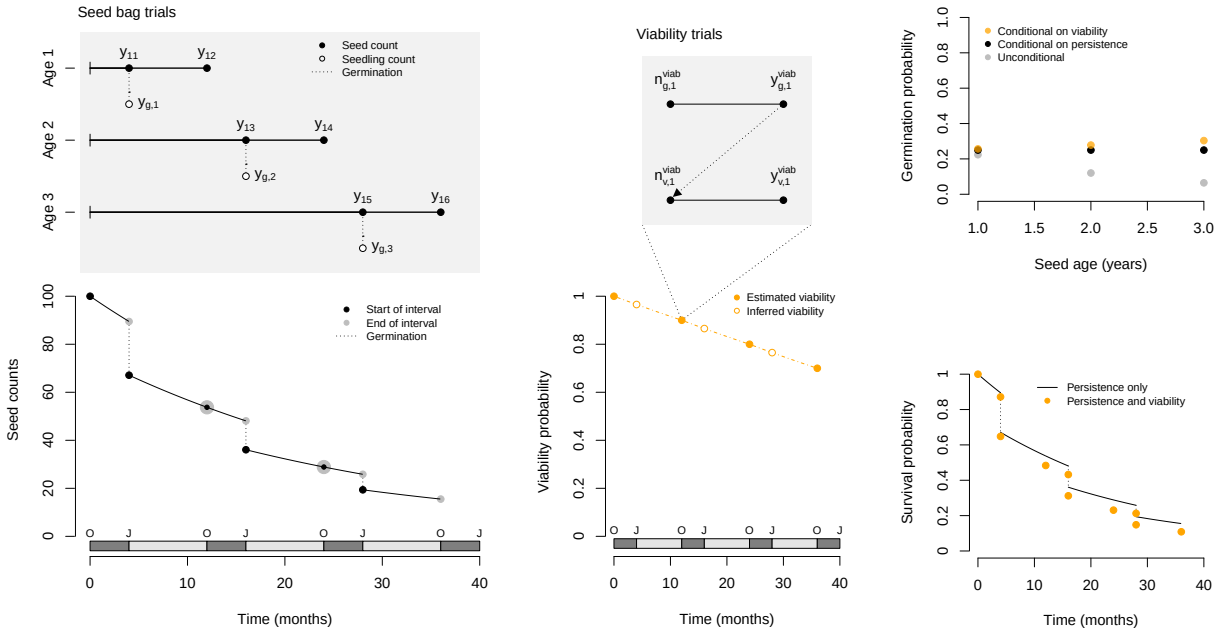

Figure 3: Summary of the seed bag burial experiments and viability trials. Figure will be labeled as (A-B: seed bag trials, C-D: viability trials, E-F: germination probability and survival probability. Add month markers to the y-axis in panels B, D, F. (A) The gray panel contains a graphical representation of the seed bag trials. Seeds were buried at the start of each experiment (100 seeds in month 0). Seed bags were unearthed and intact seeds ($y_{..}$) and germinants ($y_{g,.}$ counted. The graph below the panel shows a hypothetical survival function associated with persistence of seeds in the soil seed bank. (B) The gray panel contains a graphical representation of the viability trials. Seeds were tested in two rounds; germination trials were performed and then some or all of the ungerminated seeds were tested for viability. The graph below the panel shows hypothetical data from a series of viability trials and the interpolated, inferred viabilities at times when viability was unobserved. (C) Age-specific germination probably is summarized in three ways. (D) The graph shows the survival function for persistence of seeds in the soil seed bank (black line) and the estimated discrete survival probabilities for persistence and viability of seeds (orange points).

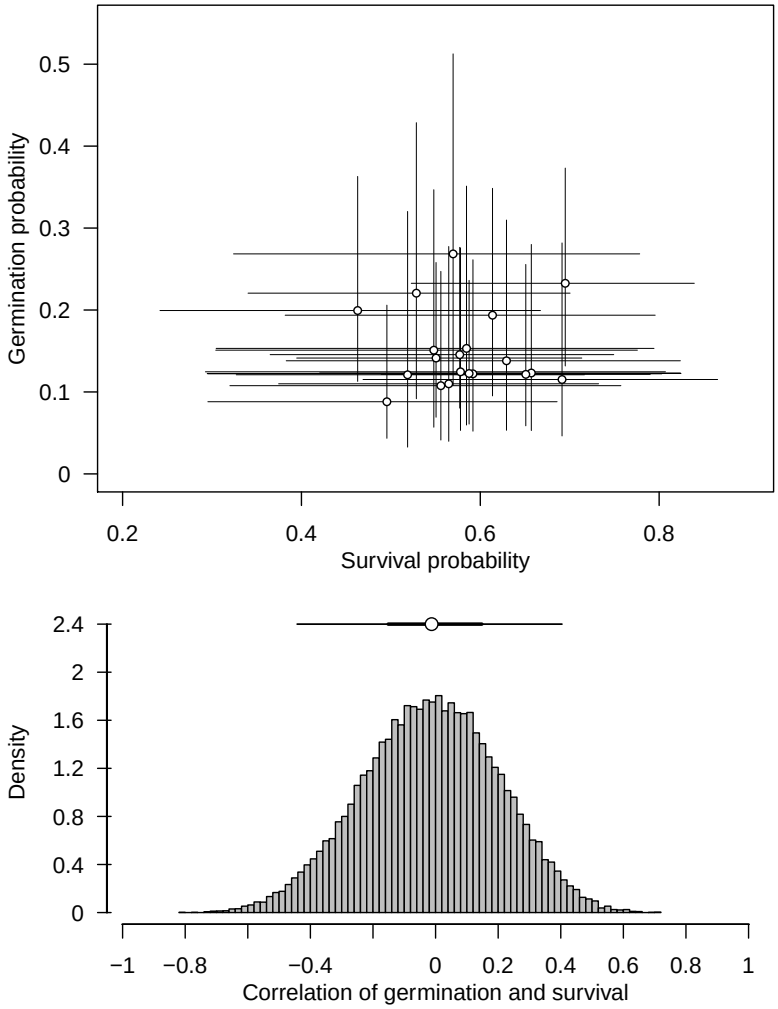

Figure 4: The top panel shows the observed germination probability plotted against probability of seed survival. The bottom panel shows the posterior distribution of correlation between observed germination probability and the probability of seed survival.

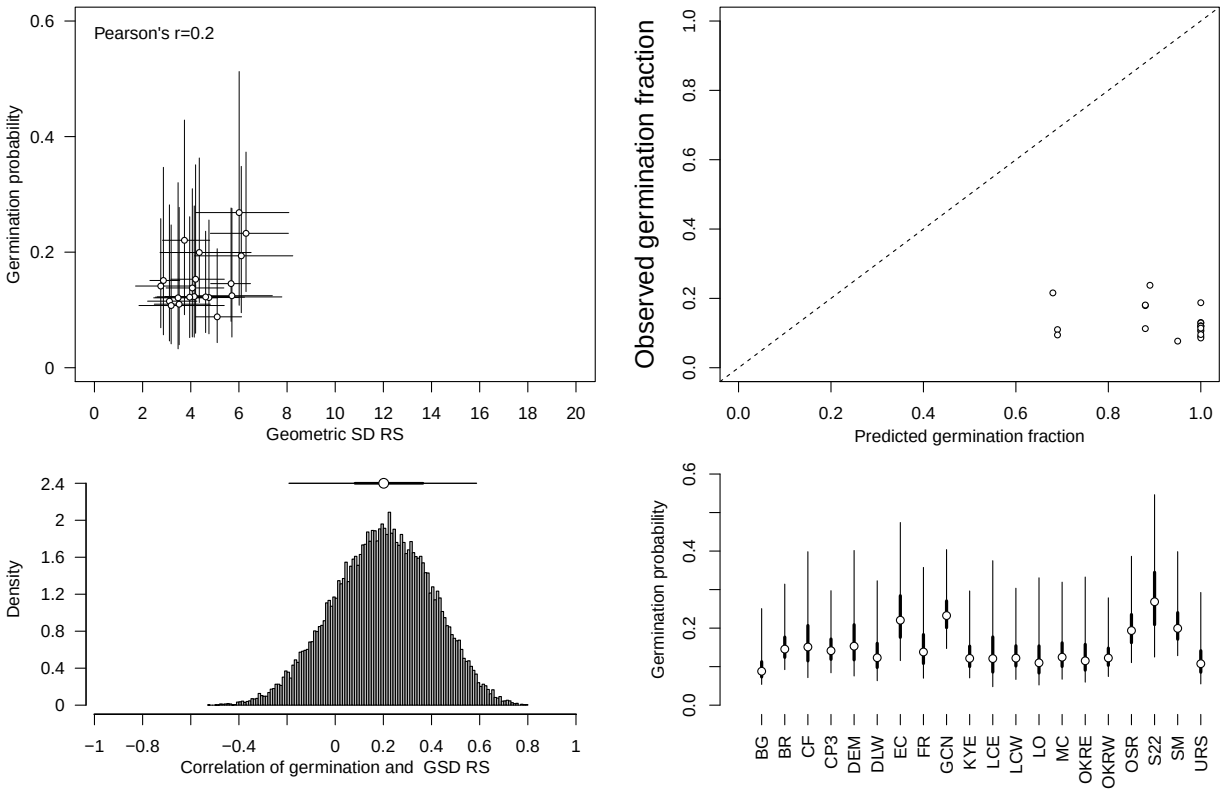

Figure 5: (A) The top left panel shows the observed germination probability plotted against the temporal variation in per capita reproductive success. (B) The bottom left panel shows the posterior distribution of correlation between observed germination probability and geometric SD of per capita reproductive success. (C) The top right panel shows observed germination probability plotted against the optimal germination probability predicted by a density-independent model. For each population, the observed germination probability is the obtained from the model for seed bank vital rates. Each point is the population-specific median of the posterior of g_1 for a model fit to data from seed bag experiments from 2006–2009. Data was pooled across years. The dotted line indicates a 1:1 relationship between observations and predictions. Values below the line indicate that the model predicts higher germination probabilities than observed; values above the line would indicate that the model predicts lower germination probabilities than observed.

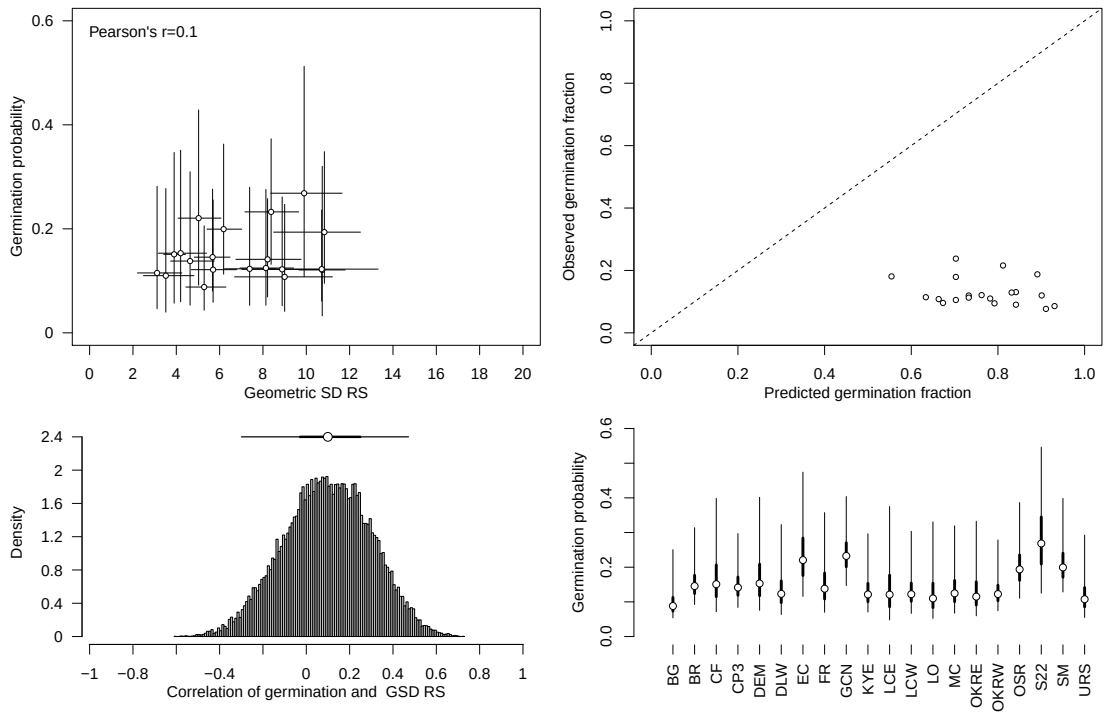

Figure 6: Results with low fitness years set to 0. (A) The top left panel shows the observed germination probability plotted against the temporal variation in per capita reproductive success. (B) The bottom left panel shows the posterior distribution of correlation between observed germination probability and geometric SD of per capita reproductive success. (C) The top right panel shows observed germination probability plotted against the optimal germination probability predicted by a density-independent model. For each population, the observed germination probability is the obtained from the model for seed bank vital rates. Each point is the population-specific median of the posterior of g_1 for a model fit to data from seed bag experiments from 2006–2009. Data was pooled across years. The dotted line indicates a 1:1 relationship between observations and predictions. Values below the line indicate that the model predicts higher germination probabilities than observed; values above the line would indicate that the model predicts lower germination probabilities than observed.

References

Cohen, D. 1966. Optimizing reproduction in a randomly varying environment. Journal of Theoretical Biology, **12**:119–129.

Cohen, D. 1967. Optimizing Reproduction in a Randoruly Varying Environment when a Correlation May Exist between the Conditions at the Time a Choice has to be Made and the Subsequent Outcome. Journal of Theoretical Biology, **16**:1–14.

Cohen, D. 1968. A General Model of Optimal Reproduction in a Randomly Varying Environment. The Journal of Ecology, **56**:219.

Eager, E. A., R. Rebarber, and B. Tenhumberg. 2014. Modeling and Analysis of a Density-Dependent Stochastic Integral Projection Model for a Disturbance Specialist Plant and Its Seed Bank. Bulletin of Mathematical Biology, **76**:1809–1834.

Easterling, M. R. and S. P. Ellner. 2000. Dormancy strategies in a random environment: Comparing structured and unstructured models. Evolutionary Ecology Research, **2**:387–407.

Eckhart, V. M., M. A. Geber, W. F. Morris, E. S. Fabio, P. Tiffin, and D. A. Moeller. 2011. The Geography of Demography: Long-Term Demographic Studies and Species Distribution Models Reveal a Species Border Limited by Adaptation. The American Naturalist, **178**:S26–S43.

Ellner, S. 1985*a*. ESS germination strategies in randomly varying environments. I. Logistic-type models. Theoretical Population Biology, **28**:50–79.

Ellner, S. 1985*b*. ESS germination strategies in randomly varying environments. II. Reciprocal Yield-Law models. Theoretical Population Biology, **28**:80–116.

Evans, M. E. K. and J. J. Dennehy. 2005. Germ Banking: Bet-Hedging and Variable Release From Egg and Seed Dormancy. The Quarterly Review of Biology, **80**:431–451.

Gremer, J. R., S. Kimball, and D. L. Venable. 2016. Within-and among-year germination in Sonoran Desert winter annuals: bet hedging and predictive germination in a variable environment. Ecology Letters, **19**:1209–1218.

Gremer, J. R. and D. L. Venable. 2014. Bet hedging in desert winter annual plants: optimal germination strategies in a variable environment. Ecology Letters, **17**:380–387.

Heinrich, L., J. Müller, A. Tellier, and D. Živković. 2018. Effects of population- and seed bank size fluctuations on neutral evolution and efficacy of natural selection. Theoretical Population Biology, **123**:45–69.

Mccue, K. A. and T. P. Holtsford. 1998. Seed bank influences on genetic diversity in the rare annual Clarkia springvillensis (Onagraceae). American Journal of Botany, **85**:30–36.

Nunney, L. 2002. The Effective Size of Annual Plant Populations: The Interaction of a Seed Bank with Fluctuating Population Size in Maintaining Genetic Variation. The American Naturalist, **160**:195.

Paniw, M., P. F. Quintana-Ascencio, F. Ojeda, and R. Salguero-Gómez. 2017. Accounting for uncertainty in dormant life stages in stochastic demographic models. Oikos, **126**:900–909.

Ritland, K. 1983. The joint evolution of seed dormancy and flowering time in annual plants living in variable environments. Theoretical Population Biology, **24**:213–243.

Venable, D. L. 2007. Bet hedging in a guild of desert annuals. Ecology, **88**:1086–1090.

Waples, R. S. 2006. Seed Banks, Salmon, and Sleeping Genes: Effective Population Size in Semelparous, Age-Structured Species with Fluctuating Abundance. The American Naturalist, **167**:118.

Supplementary material

Data summary.

Summary tables for all datasets used in the manuscript. The document summarizes the types of data collected. The document provides a table summarizing each dataset (e.g. sample size per each site and year). Link to document: https://github.com/gregor-fausto/clarkiaSeedBanks/blob/master/products/tables/data-summary.pdf

Joint posterior.

Expression for the posterior proportional to the joint distribution, and corresponding directed acyclic graphs. Link to document: https://github.com/gregor-fausto/clarkiaSeedBanks/blob/master/products/appendices/appendix-joint-posteriors/appendix-joint-posteriors.pdf

Priors.

Explanation of priors. Link to document: https://github.com/gregor-fausto/clarkiaSeedBanks/blob/master/products/appendices/appendix-priors/appendix-priors.pdf

Model checks.

Model checks, including visual posterior predictive checks and assessments with Bayesian p-values for test statistics. Link to document: https://github.com/gregor-fausto/clarkiaSeedBanks/blob/master/products/appendices/appendix-model-checks/appendix-x-model-checks.pdf